Research Square

Preprints are preliminary reports that have not undergone peer review.
They should not be considered conclusive, used to inform clinical practice,
or referenced by the media as validated information.

Transcriptome and Metabolome Analyses Reveal Key Genes potentially relative to sucrose and citrate accumulation in wampee (*Clausena Lansium Skeels*) Fruit During Fruit Advancement and Ripening

Cheng Peng
Guangdong Academy of Agricultural Sciences https://orcid.org/0000-0002-7928-0011
Xiaoxiao Chang
Guangdong Academy of Agricultural Sciences
Zhe Chen
Guangdong Academy of Agricultural Sciences
Jishui Qiu
Guangdong Academy of Agricultural Sciences
Zhixiong Lin
Guangdong Academy of Agricultural Sciences
Yusheng Lu (luyusheng@gdaas.cn)
Guangdong Academy of Agricultural Sciences

Research article

Keywords: Clausena lansium Skeels, metabolome, transcriptome, sucrose, citrate

Posted Date: October 5th, 2020

DOI: https://doi.org/10.21203/rs.3.rs-64409/v1

License: This work is licensed under a Creative Commons Attribution 4.0 International License. Read Full License

Abstract

Background: The seedless *Clausena lansium* Skeels, belonged to the *Rutaceae Clausena* family, is the main commercial variety in *China* currently. The high citrate contents in mature fruit have seriously restricted the development of the industry. The dynamic changes of sucrose and citrate, as well as the involved key regulatory genes or metabolism pathways during the fruit development of seedless wampee, however, remain unclear.

Results: In this study, we used the seedless wampee fruits at various advancement levels as materials and specified a total of 623 compounds by widely targeted metabolome. Metabolome analysis further revealed that sucrose was gradually accumulated throughout the fruit development, while citrate was accumulated rapidly in the transitionary period from fruit expansion to color conversion, and decreased slowly after color conversion period without significant difference. Moreover, we identified several key differentials expressed genes existed in sucrose as well as citrate metabolism, that mainly encode insoluble acid invertases (IVR), sucrose-phosphate synthase (SPSs), sucrose synthase (SuSy), NAD-dependent malate dehydrogenase (NAD-MDH), trehalose 6-phosphate synthase (TPS), and ATP citrate lyase (ACL), by comparing the transcriptome data of fruit in each stage.

Conclusions: We found that sucrose content was mainly regulated by *SUS, IVR, SPS,* and *TPS*, the citrate synthesis was mainly regulated by *MDH*, and the decomposition of citrate was mainly controlled by *ACLβ* in the acetyl-CoA pathway, suggesting that GABA shunt pathway did not play a decisive role.

Background

The ratio of soluble sugars to organic acids, which depends on the regulation of key genes in sugar and acid metabolism, is an essential criterion in the flavor of ripen fruits [1, 2]. Fruit advancement is regularly along with the metabolism amassment of organic acids and sugars [3–5]. However, the key regulatory genes existed the metabolism of sugars as well as organic acids have not been fully identified [6–7].

Clausena lansium Skeels (wampee), belongs to *Rutaceae Clausena*, is mainly distributed in *Asia, Oceania*, and *America*. In *South China*, it only has the commercial cultivation with an area of 10,000 hectares, and the main variety for calculation is the seedless wampee [8], which has been very popular with consumers due to the sweet-sour taste and unique flavor.

Prior investigations primarily concentrated on functional compounds of wampee, including clausenamide [9], carbazole alkaloids [10] and essential oils [11]. Over the recent years, numerous studies were earmarked to the neuroprotective capability of wampee leaf extract for improving memory as well as the treatment of *Parkinson's and Alzheimer's* diseases [12]. Wampee fruit was reported to contain sucrose and citrate as the main sugar and acid [13], respectively. However, investigation on the sucrose and citrate metabolism of wampee during fruit development remains elusive.

As an important economic crop in *China*, high citrate content in mature wampee fruit has severely restricted the development of the industry, and the appropriated sugar-acid ratio in fruit has always been the goal pursued by breeders. In the present investigation, the analyses of transcriptome and metabolome were carried out to investigate the pathway of sucrose and citrate metabolism during fruit development, in order to characterize the key genes or fundamental trajectories, thereby exploring the potential pathways for regulating the citrate content in mature fruits.

Results And Discussion

The basis quality analysis of wampee fruit in different development stages

The advancement and growth of wampee fruit could be separated into five steps: cell proliferation and differentiation, expansion (PDQ stage), coloring (ZSQ stage), fruit ripening (CSQ stage), and delay harvest (WSQ stage). This study mainly focused on the changes of seedless wampee fruit during the four stages (PDQ to WSQ stage, Fig. 1). The fruit development of seedless wampee required a 120-day cycle from flowering to fruit maturation.

According to the analysis of fruit development during four stages (Table 1), we found that total acid increased rapidly from 0.09 mg/g FW to 2.34 mg/g FW (PDQ to ZSQ stage), and decreased to 1.50 mg/g FW (ZSQ to CSQ stage), and further reduced to 1.22 mg/g FW (CSQ to WSQ stage). While the total sugar content gradually increased from 27.55 mg/g FW to 104.83 mg/g FW (CSQ to WSQ stage), which was different from total acid. These results demonstrated that the total sugar content gradually increased during the four stages, while the total acid content quickly increased in the early stages (PDQ to ZSQ stage) but maintained a relatively high level after ZSQ stage.

Metabolomics analysis

To explore the quality-related metabolism changes of seedless wampee fruit during development, we detected a number of both primary and secondary metabolites through widely targeted metabolome for the samples at the four stages (PDQmeta, ZSQmeta, CSQmeta, and WSQmeta). A total of 623 metabolites were identified(Supplement 1), containing 158 flavonoids, 81 amino acids and amino acids its subcategories, 58 fatty acids, 57 organic acids and its subcategories, 49 nucleotides and its subcategories, 31 hydroxycinnamic acid its subcategories, 21 quinic acid and its subcategories, 20 sugar, 15 plant hormones, 14 catechins and its subcategories, 14 vitamins, 13 phenolamines, 12 coumarin and its subcategories, 11 benzoic acid its subcategories, 7 indole and its subcategories, 6 choline, 6 pyridine and alcohol, 6 tryptamine and its subcategories, 6 alkaloids, 4 hydrochloric acid and its subcategories, and 3 terpenes .

By comparing the metabolome data in different development stages, 222, 156, and 104 down-regulated metabolites could be observed between PDQmeta and ZSQmeta, ZSQmeta and CSQmeta, CSQmeta and WSQmeta, respectively. From the PDQ stage to ZSQ stage, the most variable substances were flavonoids (43), amino acids (41), lipids (25), organic acids and its subcategories (23), nucleotides and its subcategories (21), carbohydrates (6), and vitamins (5). From the ZSQ stage to the CSQ stage, the most variable substances were flavonoids (24), amino acids (8), lipids (20), organic acids and its subcategories (12), nucleotides and its subcategories (13), carbohydrates (2), and vitamins (1). From the CSQ stage to the WSQ stage, the most variable substances were flavonoids (24), amino acids (7), lipids (20), organic acids and its subcategories (12), nucleotides and its subcategories (13), carbohydrates (2), and vitamins (1).

RNA-Seq and differentially expressed genes (DEGs) studies

To explore the mechanism of metabolic changes in different stages of seedless wampee fruit, especially the mechanism of sucrose and citrate changes, four transcriptome databases (PDQseq, ZSQseq, CSQseq, WSQseq) were established by RNA-sEq. The signals that were larger than 240 million could be detected in each transcriptome data library. The results showed that a total of 7191618051nt of RNA fragments were detected in PDQ stage, of which GC content accounted for 44.11%, 7392980402nt of for ZSQ stage(44.35% GC content), 7270067923nt for CSQ stage(44.25% GC content), and 7487257723nt for WSQ stage(44.43% GC content) (Table 4). According to the analysis of annotation database, such as the annotation COG, GO, KEGG, KOG, Pfam Annotation, Swissprot, eggNOG, NR, a total of 82673 unigenes were thoroughly analyzed, and the number of unigenes with a length over 1000 bp was 21781, and the number of unigenes with a length between 300 and 1000 was 34764. All RPKM values of unigene were shown in Supplement 2.

By comparing different transcriptome data library, 2540 down-regulated and 1134 up-regulated differential genes have ascertained among PDQseq and ZSQseq, 837 down-regulated and, 568 up-regulated differential genes were identified between ZSQseq and CSQseq, and 272 up-regulated and 837 down-regulated differential genes were identified between CSQseq and WSQseq (Fig. 2A). The Venn diagram of differential genes between different databases showed the total of 19 up-regulated (Fig. 2B) and 89 down-regulated differential genes (Fig. 2C) in different developmental stages.

Based on the co-expression analysis, the total of 5722 differentially expressed genes have divided into four categories, containing 452, 705, 1837 and 2728 genes in each group respectively. Group A included the up-regulated genes (Fig. 3A), and Group B included the down-regulated genes (Fig. 3B), while group C and D included the unchanged genes (Fig. 3C, 3D). Since the changed genes were involved in many metabolism pathways, we classified these genes into different pathways by KOG database according to the investigation of genes with up and down regulation, of which energy generation and transfer (C), amino acid metabolism and transport (E), secondary metabolites synthesis, metabolism and transport (Q) were the main classifications, and the sum of down-regulated genes in the aforementioned trajectories was significantly higher than the sum of up-regulated genes,

indicating that the content of energy storage substances (sucrose and glucose), amino acids and secondary metabolites (flavonoids) changed significantly during fruit development of seedless wampee.

According to the annotated genomic information of the genes that related to sucrose and citrate metabolism (shown in Table 4 and Table 5), we predicted the location information and the ratio of the expression level at each stage (the ratio > 1 means up-regulation; the ratio < 1 means down-regulation). Among all the genes, nine genes were selected from the expression profile to verify by qRT-PCR with three biological replicates for each gene. Linear analysis showed that the correlation between transcriptome data obtained by RNA-seq and gene expression levels acquired through qRT-PCR, indicating that transcriptomic data was authentic, as well as reliable (Fig. 4).

Regulation of sucrose metabolism

Fruit sucrose content mainly depends on sink strength. Sucrose is absorbed and assimilated by various organs, and it depends on the activity of enzymes (e.g., SPS, SUS, IVR [14–17]) in the sucrose metabolism pathway [18]. Here, the transcriptome data (see Table 4) showed that three *SPS* genes, five *SUS* genes, four *IVR* genes and four *TPS* genes could be detected. As shown in Fig. 5, with the maturation of wampee fruit, the sucrose and glucose content gradually augmented, which was in agreement with the cumulative trend of sucrose, glucose in other fruits, such as peach [3], pomelo [4], and watermelon [19].

From PDQ stage to ZSQ stage, the increase of sucrose content was mainly due to the up-regulation of *SUS* gene, leading to a larger amount of sucrose synthesis compared to its degradation caused by up-regulation of *IVR* gene expression. *SPS* can regulate the sucrose synthesis, and *SUS* is able to catalyze sucrose in order to produce fructose and UDP-glucose [17]. During this stage, *SPS* (c31711.graph_c0) was up-regulated by 2.11-folds, *SUS* (c49920.graph_c0, c60779.graph_c0) was up-regulated by 4.5-folds and 30.9-folds, respectively. While, the expression level of *IVR* and *TPS* did not change significantly. Besides, the sucrose content was increased by 2.05-folds, the glucose content was increased by 1.41-folds, while the Trehalose-6P content did not change. These results indicated that the synthesis rate of sucrose was much higher than the degradation rate. Also, the expression level of *HXK*, a gene involved in glycolysis, and *PEPCK* [20], a gene related to the gluconeogenesis, were up-regulated, and the content of Fructose-6P was reduced by 55%, suggesting that the respiration of wampee fruit gradually enhanced from the PDQ stage to ZSQ stage, and the precursors and energy generated by the TCA cycle increased rapidly, providing a material basis and energy for fruit expansion.

The increase rate of sucrose content slowed down during the transitionary period from ZSQ stage to CSQ stage, which might be due to the increased degradation of sucrose caused by upregulation of *IVR*, *SUS* and *TPS* genes. During this period, the upregulation of *SUS* promoted the decomposition of sucrose into fructose and UDP-glucose, while, the upregulation of *TPS* contributed to further increasing the Trehalose-6P content. The upregulation of *IVR* caused the decomposition of sucrose into fructose, which could be further transformed into Fructose-6P via down-regulating *FRK*. The metabolome database showed that the increase of sucrose (only 66%) and glucose (only 29%) gradually slowed down, while trehalose-6-phosphate, fructose-6-phosphate, and glucose-6-phosphate improved by 81%, 55%, and 37%, respectively, suggesting that some sucrose was converted into monosaccharides, which was further converted into other precursors through TCA cycle to provide energy during this period.

During the period from CSQ stage to WSQ stage, sucrose was further reduced which might be due to slower synthesis and further increased consumption rate. During this period, sucrose content, glucose, fructose-6-phosphate, glucose-6-phosphate, trehalose-6-phosphate increased by 36%, 33%, 64%, 29%, 21%, respectively. Transcriptomic data exhibited that the expression level of *SPS* was unchanged and the *SUS* gene was up-regulated during this period, suggesting that sucrose synthesis was further reduced compared to the stage before maturation. The upregulation of *IVR* involved in sucrose degradation indicated the increase of sucrose consumption. The expression of *IVR* increased rapidly from PDQ stage to ZSQ stage, then became stable. It has been reported that the acidic IVR activity of citrus fruit was activated before maturation, and then gradually disappeared due to higher fruit pH (> 5) during the CSQ stage [21–22]. While the pH of seedless wampee fruit has been maintained between pH 3 and 5 throughout the development (Table 1), indicating acidic *IVR* activity maintained a high activity throughout the development. Hence, degradation amount of sucrose from the CSQ stage to WSQ stage was the same with the period from ZSQ stage to CSQ stage, while the expression of sucrose synthesis-related genes (*SPS*, *SUS*) was lower than the period before the CSQ stage, leading to a reduced synthesis (only 36%).

According to the transcriptome and metabolome analysis, sucrose content was mainly regulated by *SUS*, *IVR*, *SPS* and *TPS* during the maturation of wampee fruit. Among these genes, synthesis related genes, such as *SUS* and *SPS* were mainly responsible for the period from PDQ stage to ZSQ stage, and the degradation-related genes, such as *IVR* and *TPS* mainly functioned after ZSQ stage.

Regulation of citrate metabolism

To explore the citrate mechanism in seedless wampee fruit, transcriptome and metabolome analyses were used to analyze fruit citrate metabolism-related genes and pathways during fruit development (Fig. 6). From PDQ stage to ZSQ stage, *MDH* expression increased significantly, citrate content increased by 35%, while malic acid content decreased by 66%. These findings indicated that citrate synthesis and malic acid decomposition were positively correlated with *MDH* expression, which was most likely due to the upregulation of *MDH* that promote the malic acid to be oxidized by NAD-mtMDH, and further being converted into citrate via pyruvate and stored in vacuole. Besides, there was no differential expression for citrate synthase gene, suggesting the synthesis of citrate in wampee fruit might be regulated by *MDH* but not citrate synthase gene [4, 23].

After the ZSQ stage, the citrate content decreased slowly, indicating only part of citrate was converted into other substances after transporting out of the vacuole. Generally, the conversion of citrate into other substances was mainly through TCA cycle, glyoxylate cycle, GABA shunt, and acetyl-CoA catabolism [24]. The TCA cycle might not determine the citrate content of wampee fruit. After the ZSQ stage, the malic acid content gradually decreased, the content of fumaric acid did not change significantly, and other genes in TCA cycle, such as citrate synthase gene, isocitrate dehydrogenase gene, and *cis*-aconitate gene, were also not significantly differentially expressed. Also, it has been reported that citrate could be transported out of the mitochondria in the TCA cycle [25], implying the TCA cycle was closely related to the decomposition of fruit citrate but cannot determine the citrate content [26–27]. Here, the transcriptome data showed that the key gene ICL was not differentially expressed in glyoxylate cycle pathway, indicating that the degradation of citrate was not involved in this pathway. GABA shunt and acetyl-CoA pathways are the main decomposition trajectories for citrate during fruit ripening such as banana [28], tomato [29], and orange [30]. Here, we found that after ZSQ stage, the expression of *ACO* and *IDH (not detected)*, key genes in GABA shunt pathway, did not change significantly (Table 5), and the content of glutamic acid, glutamine, asparagine in the pathway gradually decreased. These findings strongly suggested that the GABA shunt pathway might not be the main pathway for citrate decomposition after ZSQ stage. The acetyl-CoA pathway is mainly involved in the decomposition of citrate during fruit maturation [31]. In this pathway, *ACL*, a key gene in acetyl-CoA pathway, could generate oxaloacetic acid and acetyl-CoA by catalyzing citrate, and finally generate fatty acids, amino acids, and flavonoids. Here, the expression of *ACLβ* was negatively correlated with citrate content, suggesting that the acetyl-CoA pathway might be the main pathway for citrate decomposition after the ZSQ stage (Fig. 6).

Conclusions

The widely targeted metabolome has been widely used in rice [32], citrus [33], and potato [34]. Here, we identified and annotated a total of 623 compounds of wampee fruits in different development stages, mainly for flavones, saccharides, amino acids and organic acids.

Wampee has been very popular with consumers due to their abundant polyphenol and other beneficial substances, but high citrate content in mature fruit seriously restricts the development of the industry. Nevertheless, there were still little reports on differential metabolisms and genes of seedless wampee fruits in different developmental stages. Therefore, this study mainly focused on the differential mechanisms of metabolites during the fruit development of wampee fruits, especially sucrose and citrate. The transcriptome data showed that the differential genes mainly involved in energy production and transfer (C), amino acids translocation and metabolism (E), secondary metabolites synthesis, translocation and metabolism (Q) during fruit development, suggesting that the metabolite content of sucrose and organic acids in these pathways significantly changed. The transcriptome and metabolome analyses further showed that sucrose content, which might be mainly regulated by genes such as *SUS*, *IVR*, *SPS*, and *TPS*, was gradually accumulated throughout fruit development with gradually decreased accumulation amount. While the citrate content was increased firstly and then slowly decreased. Also, its synthesis might be mainly regulated by *MDH*, and its decomposition might be dominated by the acetyl-CoA pathway, suggesting that the GABA shunt pathway cannot determine citrate content.

Methods

Plant materials

Wampee trees grow in the Wampee Resource Nursery of the Ministry of Agriculture (Guangzhou). All the wampee trees used in this experiment were planted in 2008. The branches were planted with a spacing of 3 to 4 m, and all the lines were heading north to south. Fertilizer and water management and pest control were performed according to the resource nursery management manual of the Ministry of Agriculture. Fruits were harvested during the wampee developing and ripening season in 2018. Each sample constituted 120 fruits from three trees with the same size and color in expansion (PDQ stage, 50DAF), coloring (ZSQ stage, 70DAF), fruit ripening (CSQ stage, 91DAF), and delay harvest (WSQ stage, 100DAF). After the samples were randomly divided into three replicates and stored at -80 ℃ for further use.

pH, Total acid (TA) and Total soluble sugars

pH was evaluated utilizing a digital hand-held refractometer (pHS-25, Shanghai). Three droplets of juice attained *via* one fragment were evaluated, and the process was iterated two times to per fruit and with 12 individual fruit repeats. Total soluble sugars(TSS) concentrations were determined by the phenol-sulfuric acid method. Following the aforementioned evaluation, the remained fragments were separated into three categories. Each category of separated fragments was selected from four fruits, and also 5 ml of juice from each one of the categories was diluted well in 20 ml distilled water and then by using 0.1 N NaOH was titrated at pH 8.2 as the ending point conforming to the approach already published [35]. Total acid (TA) as a percentage of citric acid was measured.

Metabolome analysis

The MRM was carried out *via* Metware Biotechnology Co., Ltd. (Wuhan, China). The exterior shell of spears which are dried in a frozen form were all pulverized by utilizing a blender mill (MM 400, Retsch) that contains zirconia beads at 30 Hz for 1.5 min. The weight measurement of 100 mg powder was performed and then extracted over the nightlong at 4 °C using 1.0 mL of 70% aqueous methanol. Following 10 min centrifugation at 10,000 × g, the attained extracts were completely absorbed and subsequently filtered. Afterward, the extracts of the specimen were characterized by implementing an LC-ESI-MS/MS system (HPLC, Shim-pack UFLC Shimadzu CBM30A system, www.shimadzu.com.cn/; MS, Applied Biosystems 6500 Q TRAP, www.appliedbiosystems.com.cn/). The considered analytical circumstances are consisted of: HPLC: column, Waters ACQUITY UPLC HSS T3 C18 (1.8 μm, 2.1mm* 100 mm); the system of solvent, aqueous medium (0.04% acetic acid): acetonitrile (0.04% acetic acid); gradient program, 100:0 V/V at 0 min, 5:95 V/V at 11.0 min, 5:95 V/V at 12.0 min, 95:5 V/V at 12.1 min, 95:5 V/V at 15.0 min; flow rate, 0.40 mL/min; temperature, 40 °C; injection volume: 2 μl. The sewage was linked as an alternative to the system of ESI-triple quadrupole-linear ion trap (Q TRAP)-MS. The scans of triple quadrupole (QQQ), as well as Linear ion trap (LIT), were achieved through an API 4500 Q TRAP LC/MS/MS system, supplied with an ESI Turbo Ion-Spray interface, performing in a mode of positive ion and monitored with an Analyst 1.6 software (AB Sciex). For the ESI resource, the following process criteria were considered: ion source, turbospray; source temperature, 500 °C; and ion spray voltage (IS) voltage, 5500 V. Furthermore, the ion source gas I (GSI), gas II (GSII), and curtain gas (CUR) have adjusted at 55, 60, and 25.0 psi, respectively, and the gas of collision (CAD) has adjusted at great values.

Mass calibration as well as Instrumental tuning have executed with 10 and 100 μmol/L polypropylene glycol solutions in the modes of LIT and QQQ, respectively. QQQ scans were obtained in the time of MRM assessments within collision gas (nitrogen) adjusted to 5 psi. DP and CE for separate MRM transitions have fulfilled with considering the subsequent optimization of DP and CE. A particular sort of MRM transition has observed for each time course conforming to the metabolites eluted through the specific time. The MRM for each cultivar has replicated three times. Three spears were utilized for each replication.

RNA-seq and Annotation

The total amount of utilized RNA per specimen was 3 μg, which was used as an input substance for the preparation of RNA specimen. It is worth to point that the minimum of three biological replications have assembled and blend simultaneously. The act of RNA-seq assembly and sequencing was accomplished *via* Biomarker Technology Co. (Beijing, China). The sequencing libraries were created through utilizing NEBNext® Ultra™ RNA Library Prep Kit for Illumina® (NEB, USA) and taking advantage of

manufacturer's suggestions and criteria codes to allocate sequences to each specimen. The first strand of cDNA was prepared by utilizing random hexamer primer as well as M-MuLV Reverse Transcriptase(RNase H^-). Further, the preparation of Second strand cDNA has done by utilizing RNase H and DNA Polymerase I. Through the exonuclease/polymerase activities, remaining overhangs were transformed into flat ends. Following the adenylation of 3' ends of DNA segments, the adaptor of NEBNext containing hairpin loop configuration was illuminated in order to be prepared for hybridization. In continue, 3 µl USER Enzyme (NEB, USA) has implemented with the scale-selected, ligated adaptor cDNA for 15 min at 37 °C and extended at 95 °C for 5 min prior PCR. Then PCR was exerted within Phusion High-Fidelity DNA polymerase, Universal PCR primers as well as Index (X) Primer. Eventually, the products of PCR have completely purified (AMPure XP system) and the quality of the library has evaluated on the system of Agilent Bioanalyzer 2100. The clustering procedure of the index-coded specimen was exerted on a system of cBot Cluster Generation by implementing TruSeq PE Cluster Kit v3-cBot-HS (Illumina) conforming to the manufacturer's instructions. Following the cluster creation, the prepared library was sequenced on a platform of Illumina Hiseq 2000 and paired-end reads were created. The annotation of gene functions has done according to the following database: NR (NCBI non-redundant protein sequences); Pfam (Protein class); KOG/COG/eggNOG (Clusters of Orthologous Groups of proteins); Swiss-Prot (A manually annotated and reviewed protein sequence database); KEGG (Kyoto Encyclopedia of Genes and Genomes); GO (Gene Ontology).

Investigation of the Differentially Expressed Genes(DEGs)

DESeq R package (1.10.1) was used for a meticulous investigation of differential expression analysis for two conditions/groups. DESeq is capable to represent statistical routines for ascertaining differential expression in digital gene expression data by utilizing a model founded on the negative binomial distribution. The calculated P values were modified by utilizing Hochberg and Benjamini's method for monitoring the rate of incorrect discovery. The genes with an tuned P-value < 0.05 based on DESeq were determined as differentially expressed.

qPCR Validation

RNA extraction as well as quality evaluation was accomplished *via* RNASEq. Reverse transcription was carried out by utilizing HiFi-MMLV cDNA First-Strand Synthesis Kit (Invitrogen). For RT-qPCR, nine genes were picked within particular primers (Supplement 3) created by Primer Premier 5 software. The RT-qPCR was done with a detection system of ABI 7500 Fast Real-Time (Applied Biosystems) utilizing the Ultra SYBR Mix kit (CWBIO, Beijing, China). The system of amplification was formed from 10.4 µL Ultra SYBR Premix System II, 0.8 µL of 10 µmol/L upstream primer, 0.8 µL of 10 µmol/L downstream primer, 2 µL template, and sterile distilled water to a whole volume of 20 µL. The program of amplification was fulfilled for 10 min at 95◦C, succeeded by 40 cycles of 95◦C for 15 s and, 55◦C for 1 min. corresponding quantitative investigation of data was carried out through the $2^{-\triangle\triangle CT}$ approach within the reference genes actin-7. Three technical replications were implemented for each specimen to certify the reliability and reproducibility. Statistical investigation of variance (ANOVA) and Duncan's novel multiplex span tests were executed with SPSS Version 16.0 (Chicago, IL, USA). The significance level was adjusted to $P < 0.05$.

Abbreviations

PDQ stage (fruit expansion); ZSQ stage (fruit coloring); CSQ stage (fruit ripening); WSQ stage (fruit delay harvest); PDQmeta(fruit expansion stage metabolome databases); ZSQmeta(fruit coloring stage metabolome databases); CSQmeta(fruit ripening stage metabolome databases); WSQmeta(fruit delay harvest stage metabolome databases); PDQseq(fruit expansion stage transcriptome databases); ZSQseq(fruit coloring stage transcriptome databases); CSQseq(fruit ripening stage transcriptome databases); WSQseq(fruit delay harvest stage transcriptome databases); IVR(insoluble acid invertases);SPSs(sucrose-phosphate synthase); SuSy(sucrose synthase);NAD-MDH (NAD-dependent malate dehydrogenase); TPS(trehalose 6-phosphate synthase); ACL (ATP citrate lyase); NR (NCBI non-redundant protein sequences); Pfam (Protein class); KOG/COG/eggNOG (Clusters of Orthologous Groups of proteins); Swiss-Prot (A manually annotated and reviewed protein sequence database); KEGG (Kyoto Encyclopedia of Genes and Genomes); GO (Gene Ontology).

Declarations

Ethics approval and consent to participate

Not applicable. The authors declared that experimental research works on the plants described in this paper comply with institutional, national and international guidelines.

Consent for publication

Not applicable.

Availability of data and material

The datasets supporting the conclusions of this article are included within the article and its additional files.

Competing interests

The authors of this research announce that they have no competing interests.

Funding

This work was supported by Guangdong Academy of Agricultural Sciences President Fund (201817), Guangdong modern Agro-industry technology Research System (2019KJ116), Guangdong Provincial Crops Germplasm Nursery Construction and Resources, Collection, Preservation, Identification&Evaluation, National Tropical Plants Germplasm Resource Center and Foshan Municipal Special Financial Fund – 2019 Co-construction project of Guangdong Agricultural Science and Technology Demonstration City.

Author's contributions

C.P. and Z.C. represented the main idea and designed the assessments; X.C. and Y.L. carried out the assessments; J.P., Z.L. and J.Q. provided materials/ reagents/ analysis equipment; C.P. was the author.

Author details

[1] Institute of Fruit Tree Research, Guangdong Academy of Agricultural Sciences; Key laboratory of South Subtropical Fruit Biology and Genetics Resource Utilization, Ministry of Agriculture; Key Laboratory of Tropical and Subtropical Fruit Tree Research, Guangzhou 510640, China.

References

1. Kader AA. Flavor quality of fruits and vegetables. J Sci Food Agric. 2008;88:1863–8.
2. Obenland D, Collin S, Mackey B, Sievert J, Fjeld K, et al. Determinants of flavor acceptability during the maturation of navel oranges. Postharvest Biol Technol. 2009;52:156–63.
3. Wu BH, Quilot B, Génard M, Kervella J, Li SH. Changes in sugar and organic acid concentrations during fruit maturation in peaches, P. davidiana and hybrids as analyzed by principal component analysis. Sci Hortic. 2005;103:429–39.
4. Lin Q, Wang C, Dong W, Jiang Q, Wang D, et al. Transcriptome and metabolome analyses of sugar and organic acid metabolism in Ponkan (Citrus reticulata) fruit during fruit maturation. Gene. 2015;554:64–74.
5. Serrano M, Zapata P, Pretel MT, Almansa MS, Botella MA. Changes in organic acid and sugars levels during ripening of five loquat (Eriobotrya japonica Lindl.) cultivars. In:Llácer G, editor, Badenes M.L, editor. First international symposium on loquat. Zaragoza : CIHEAM. 2003;p. 157–160.
6. Tadeo FR, Cercos M, Colmenero-Flores JM, Iglesias DJ, Talon M. Molecular physiology of development and quality of citrus. Advances in Botanical Research. 2008;47:147–223.
7. Terol J, Soler G, Talon M, et al. The aconitate hydratase family from Citrus[J]. BMC Plant Biol. 2010;10(1):222.
8. Lim TK. Clausena lansium. In: Edible Medicinal And Non-Medicinal Plants. Dordrecht: Springer; 2012. 871–83 p.
9. Li SH, Wu SL, Li WS. Amides and coumarin from the leaves of Clausena lansium. J Chinese Pharm Sci. 1996;48:367–73.

10. Lakshmi V, Raj K, Kapil RS. Chemical constituents of Clausena lansium: Part III - Structure of lansamide-3 and 4. Indian J Chem. 1998;37:422–4.
11. Pino JA, Marbot R, Fuentes. V.Aromatic plants from western Cuba. IV. Composition of the leaf oils of Clausena lansium (Lour.) Skeels and Swinglea glutinosa (Blanco) Merr. J Essent Oil Res. 2006;18:139–41.
12. Hu JF, Chu SF, Ning N, Yuan YH, Xue W, Chen NH, Zhang JT. Protective effect of (–)clausenamide against Aβ-induced neurotoxicity in differentiated PC12 cells. Neurosci Lett. 2010;483:78–82.
13. Sun D, Xinhua LU, Liang J, Yulin HU, Xie J. Fruit Quality and Constituent of Sugars and Organic Acids in Wampee Cultivars. Chinese Journal of Tropical Crops. 2012;33(8):1418–21.
14. Koch K. Sucrose metabolism: regulatory mechanisms and pivotal roles in sugar sensing and plant development. Curr Opin Plant Biol. 2004;7:235–46.
15. Barratt DH, Derbyshire P, Findlay K, Pike M, Wellner N, et al. Normal growth of Arabidopsis requires cytosolic invertase but not sucrose synthase. Proc Natl Acad Sci. 2009;106:13124–9.
16. Baroja-Fernandez E, Munoz FJ, Montero M, Etxeberria E, Sesma MT, et al. Enhancing sucrose synthase activity in transgenic potato (Solanum tuberosum L.) tubers results in increased levels of starch, ADPglucose and UDPglucose and total yield. Plant Cell Physiol. 2009;50:1651–62.
17. Micallef BJ, Sharkey TD. Altered photosynthesis, flowering, and fruiting in transgenic tomato plants that have an increased capacity for sucrose synthesis. Planta. 1995;196:327–34.
18. Marcelis LF. Sink strength as a determinant of dry matter partitioning in the whole plant. J Exp Bot. 1996;47:1281–91.
19. Gao L, Zhao S, Lu X, He N, Zhu H, et al. Comparative transcriptome analysis reveals key genes potentially related to soluble sugar and organic acid accumulation in watermelon. PLoS One. 2018;13:e0190096.
20. Sweetman C, Deluc LG, Cramer GR, Ford CM, Soole KL. Regulation of malate metabolism in grape berry and other developing fruits. Phytochemistry. 2009;70:1329–44.
21. Lowell CA, Tomlinson PT, Koch KE. Sucrose-metabolizing enzymes in transport tissues and adjacent sink structures in developing citrus fruit. Plant Physiol. 1989;90:1394–402.
22. Sturm A, Invertases. Primary structures, functions, and roles in plant development and sucrose partitioning. Plant Physiol. 1999;121:1–7.
23. Tang M, Bie Z-l, Wu M-z, Yi H-p, Feng J-x. Changes in organic acids and acid metabolism enzymes in melon fruit during development. Sci Hortic. 2010;123:360–5.
24. Etienne A, Genard M, Lobit P, Mbeguie AMD, Bugaud C. What controls fleshy fruit acidity? A review of malate and citrate accumulation in fruit cells. J Exp Bot. 2013;64:1451–69.
25. Katz E, Boo K, Kim H, et al. Label-free shotgun proteomics and metabolite analysis reveal a significant metabolic shift during citrus fruit development[J]. J Exp Bot. 2011;62:5367–84.
26. Deng W, Luo K, Li Z, et al. Molecular cloning and characterization of a mitochondrial dicarboxylate/tricarboxylate transporter gene in Citrus junos response to aluminum stress[J]. Mitochondrial DNA. 2008;19:376–84.
27. Regalado A, Pierri C, Bitetto M, et al. Characterization of mitochondrial dicarboxylateã/tricarboxylate transporters from grape berries[J]. Planta. 2013;237(3):693–703.
28. Chen RD, Gadal P. Structure, functions and regulation of NAD and NADP dependent isocitrate dehydrogenases in higher plants and in other organisms. Plant Physiol Biochem. 1990;28:827–9.
29. Morgan MJ, Osorio S, Gehl B, Baxter CJ, Kruger NJ, et al. Metabolic engineering of tomato fruit organic acid content guided by biochemical analysis of an introgression line. Plant Physiol. 2013;161:397–407.
30. Sadka A, Dahan E, Cohen L, Marsh KB. Aconitase activity and expression during the development of lemon fruit. Physiol Plant. 2010;108:255–62.
31. Terol J, Soler G, Talon M, Cercos M. The aconitate hydratase family from Citrus. Bmc Plant Biology. 2010;10:1–12.
32. Chen W, Gao Y, Xie W, Gong L, Lu K, Wang W, … Luo J. Genome-wide association analyses provide genetic and biochemical insights into natural variation in rice metabolism. Nat Genet. 2014;46(7):714–21.

33. Wang S, Hong T, Jian W, Wei C, Liu X, Jie L, Zhang H. Spatio-temporal distribution and natural variation of metabolites in citrus fruits. Food Chem. 2016;199:8–17.
34. Zhu G, Wang S, Huang Z, Zhang S, Liao Q, Zhang C, Lin T, Qin M, Peng M, Yang C, Cao X, Han X, Wang X, van der Knaap E, Zhang Z, Cui X, Klee H, Fernie AR, Luo J, Huang S. Rewiring of the fruit metabolome in tomato breeding. Cell. 2018;172(1–2), 249–261 e212.
35. Chen M, Xie X, Lin Q, Chen J, Grierson D, et al. Differential Expression of Organic Acid Degradation-Related Genes During Fruit Development of Navel Oranges (Citrus sinensis) in Two Habitats. Plant Molecular Biology Reporter. 2013;31:1131–40.

Tables

Table 1 Wampee cultivars used in the present study and their quality index.[a.b.c.d]

Stage.	Description	Abbreviation	TA (mg/g FW)	TS (mg/g FW)	pH
1	50DAF	PDQ	0.09±0.01d	2.76±0.72d	5.40±0.02a
2	70DAF	ZSQ	2.34±0.01a	3.62±0.23c	3.25±0.03c
3	91DAF	CSQ	1.50±0.01c	7.44±1.88b	3.72±0.04b
4	100DAF	WSQ	1.22±0.00b	10.48±2.70a	3.35±0.02c

a TS, Total sugar content. b TA, titratable acidity. c Data are expressed as means ± standard deviation of triplicate samples. d Different lowercase letters between columns represent significant differences between cultivars ($p < 0.05$).

Table2 Compounds relative content related to sucrose and citrate metabolism.					
Compounds	Index	PDQ	ZSQ	CSQ	WSQ
Organic Acid					
Citric acid	Cll842	5.29E+07	7.14E+07	6.88E+07	6.61E+07
Malic acid	Cll910	1.02E+08	3.44E+07	2.64E+07	2.41E+07
Methylmalonic acid	Cll947	1.22E+07	5.99E+06	1.10E+07	4.95E+07
γ-aminobutyric acid	Cll23	3.66E+06	5.37E+06	6.17E+06	6.88E+06
5-Aminolevulinate	Cll32	2.16E+06	2.53E+06	3.77E+06	6.84E+06
2-Methylsuccinic acid	Cll991	5.70E+06	4.82E+06	4.89E+06	6.08E+06
Argininosuccinate	Cll847	9.99E+06	1.19E+07	7.64E+06	3.53E+06
Aminomalonic acid	Cll906	5.26E+05	2.55E+05	5.15E+05	2.57E+06
Creatine	Cll820	1.89E+06	1.13E+06	1.59E+06	2.49E+06
Phosphoric acid	Cll92	2.69E+06	2.24E+06	2.13E+06	2.37E+06
Terephthalic acid	Cll1062	1.93E+06	2.09E+06	2.04E+06	2.04E+06
Succinic acid	Cll150	3.06E+05	2.41E+05	3.37E+05	1.86E+06
Oxoadipic acid	Cll932	9.00E+00	5.61E+05	8.25E+05	1.38E+06
6-Aminocaproic acid	Cll93	4.08E+05	5.06E+05	6.00E+05	1.16E+06
Shikimic acid	Cll863	2.81E+06	4.43E+05	1.10E+06	1.15E+06
Kynurenic acid	Cll1040	4.42E+05	6.34E+05	5.04E+05	7.01E+05
(Rs)-Mevalonic acid	Cll930	2.24E+06	6.94E+05	5.41E+05	6.22E+05
Glutaric acid	Cll969	3.02E+05	4.14E+05	3.40E+05	4.02E+05
4-Acetamidobutyric acid	Cll949	3.73E+05	4.11E+05	3.35E+05	3.63E+05
Fumaric acid	Cll919	4.57E+05	8.35E+04	1.01E+05	3.20E+05
Carbohydrates					
D-Melezitose O-rhamnoside	Cll810	5.40E+03	6.54E+03	9.26E+03	1.04E+04
Ribulose-5-phosphate	Cll864	9.82E+03	8.07E+03	1.24E+04	1.41E+04
D(-Melezitose	Cll51	2.39E+04	2.52E+04	1.75E+04	2.32E+04
L-Gluonic-γ-lactone	Cll829	8.69E+03	1.04E+04	1.60E+04	2.46E+04
L-Fucose	Cll855	2.17E+04	1.79E+04	3.34E+04	4.28E+04
D-Threose	Cll116	1.89E+05	8.30E+04	7.92E+04	7.90E+04
Glucosamine	Cll8	2.66E+05	2.02E+05	1.52E+05	9.63E+04
D-Glucono-1,5-lactone	Cll844	3.29E+04	4.64E+04	8.62E+04	1.03E+05
Trehalose 6-phosphate	Cll848	5.91E+04	5.87E+04	1.06E+05	1.29E+05
D-glucoronic acid	Cll839	2.47E+05	2.75E+05	2.49E+05	2.51E+05
2-Deoxyribose 1-phosphate	Cll858	1.96E+05	3.46E+04	4.93E+04	2.62E+05
DL-Arabinose	Cll841	9.50E+04	1.57E+05	2.85E+05	3.10E+05

D-Fructose 6-phosphate	Cll914	3.40E+05	1.52E+05	2.35E+05	3.86E+05
Gluconic acid	Cll777	1.02E+06	4.30E+05	3.77E+05	4.86E+05
N-Acetyl-D-glucosamine	Cll86	5.78E+05	6.23E+05	6.42E+05	6.34E+05
D-Glucose 6-phosphate	Cll860	2.70E+06	1.82E+06	2.50E+06	3.22E+06
D-Glucose	Cll819	8.85E+05	2.13E+06	2.76E+06	3.67E+06
D-Sedoheptuiose 7-phosphate	Cll922	1.35E+07	1.29E+07	8.26E+06	4.70E+06
Glucarate O-Phosphoric acid	Cll869	2.34E+07	2.62E+07	2.00E+07	9.68E+06
D-Sucrose	Cll828	1.44E+06	4.40E+06	7.31E+06	9.95E+06

Table3 Summary statistics of sequencing and assembly

Stage	Description	Abbreviation	Total reads	Total nucleotides(nt)	GC percentage
1	45DAF	PDQseq	24027588	7191618051	44.11%
2	60DAF	ZSQseq	24698261	7394980402	44.35%
3	75DAF	CSQseq	24302233	7270067923	44.25%
4	90DAF	WSQseq	24248347	7258745723	44.43%

Table 4

Gene or gene members related to sucrose metabolism.

Gene	Enzyme	Genome number	Predicted location	All	ZSQseq /PDQseq	CSQseq /ZSQseq	WSQseq /CSQseq
SPS	sucrose-phosphate synthase	c31711.graph_c0	-	3	3.11	0.19	1.27
		c57218.graph_c0	_		0.71	3.75	0.75
		c73222.graph_c0	_		1.15	2.88	0.71
SUS	sucrose synthase	c42806.graph_c0	-	4	-	0.04	4.45
		c49920.graph_c0	S		5.69	0.19	1.76
		c60779.graph_c0	C		31.86	0.11	2.95
		c66450.graph_c1	-		0.22	5.23	0.67
IVR	invertase	c56363.graph_c0	C	4	0.05	1.35	1.7
		c61222.graph_c0	_		3.82	1.64	0.77
		c63840.graph_c0	-		2.18	1.18	1.71
		c68755.graph_c1	C		0.16	0.87	0.52
TPS	trehalose 6-phosphate synthase	c55388.graph_c0		4	0.28	0.15	0.85
		c66605.graph_c2			0.47	0.35	1.08
		c66605.graph_c3			0.47	0.43	0.61
		c67317.graph_c0			11.1	7.26	0.54
HXK	Hexokinase	c31774.graph_c0	-	2	3.7	1.16	0.76
		c58675.graph_c0	C		0.48	1.02	0.84
PFK1	6-phosphofructokinase 1	c53477.graph_c0	_	1	0.12	8.05	0.84
ALDO	fructose-bisphosphate aldolase, class I	c22154.graph_c0	-	3	266.12	-	18.17
		c35502.graph_c0	-		169.33	0.02	0.62
		c45233.graph_c0	S		0.29	3.53	0.61
TPI	triosephosphate isomerase (TIM)	c48467.graph_c0	_	2	0.34	4.67	0.46
		c48467.graph_c1	S		0.28	4.33	0.53
PGK	phosphoglycerate kinase	c63869.graph_c0	C	2	0.33	3.7	0.55
		c70507.graph_c0	C		5.43	0.17	1.28
FRK	Fructokinase	c59562.graph_c0	-	2	0.41	3.08	0.66
		c53477.graph_c1	-		0.11	8.7	0.85

C: chloroplast; S: Secretory pathway; –: uncertain.

All: all gene number;

The localization was predicted by the online tool TargetP 1.1 Server.

Table 5

Gene or gene members related to citrate metabolism and the TCA cycle.

Gene	Enzyme	Genome number	Predicted location	ALL	ZSQseq/PDQseq	CSQseq/ZSQseq	WSQseq/ CSQseq
PK	pyruvate kinase	c59774.graph_c1	-	2	1.80	0.53	0.86
		c60884.graph_c0	C		2.77	0.21	2.14
PEPCK	phosphoenolpyruvate carboxykinase (ATP)	c66743.graph_c0	-	3	2.80	0.79	1.23
		c66743.graph_c1	S		0.42	3.00	0.99
MDH	malate dehydrogenase	c51120.graph_c0	-		24.37	0.14	2.26
		c52097.graph_c0	-	1	0.08	0.27	0.52
		c60366.graph_c0	-	2	2.03	1.09	0.57
ACLβ	ATP citrate lyase beta	c56989.graph_c0	C		1.05	1.31	0.47
GS	glutamine synthetase	c32009.graph_c0	C	1	75.64	0.00	25.29
GDH	Glutamate dehydrogenase	c20196.graph_c0	-	2	6.08	0.06	2.56
		c64308.graph_c1	-	1	0.48	1.79	1.26
		c65520.graph_c0	C	3	0.41	2.39	0.53
GAD	glutamate decarboxylase	c64308.graph_c1	-	1	0.48	1.79	1.26
ACSS	acetyl-CoA synthetase	c69431.graph_c0	C	1	0.24	4.53	0.44
PDC	pyruvate decarboxylase	c21939.graph_c0	-	2	0.08	15.59	0.45
		c61395.graph_c0	-		0.18	5.58	0.54
ACO	aconitase	c45787.graph_c1	-	2	0.84	1.05	1.44
		c49397.graph_c0	-		-	-	-

C: chloroplast; S: Secretory pathway; –: uncertain.

All: all gene number;

The localization was predicted by the online tool TargetP 1.1 Server.

Figures

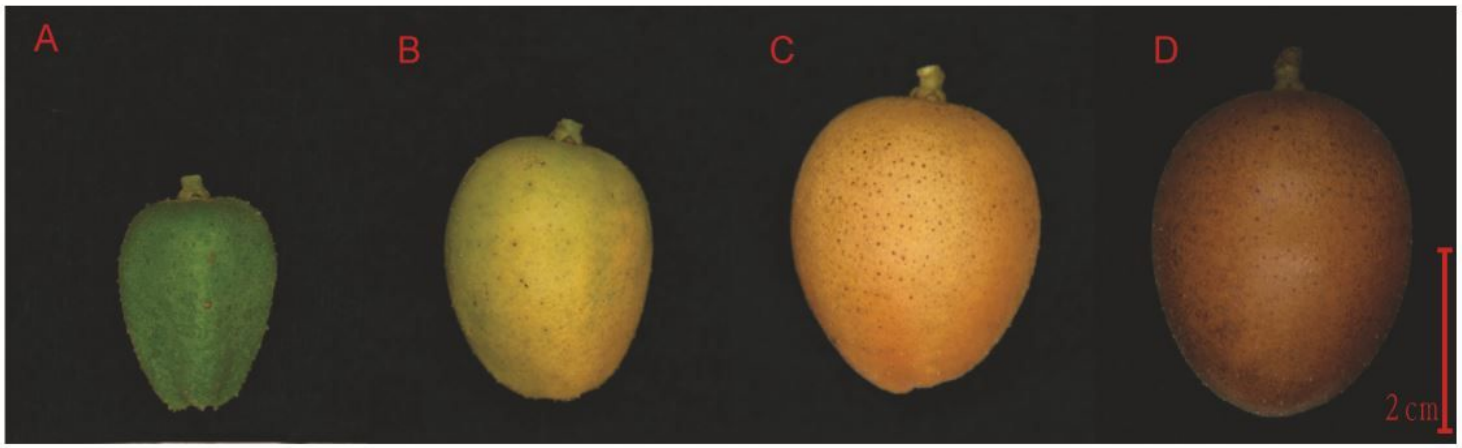


Figure 1

Developmental changes of KM fruit during growth and maturation. Fruits are shown 50 (A), 70(B), 91 (C), and 100 (D) days after flowering(DAF).

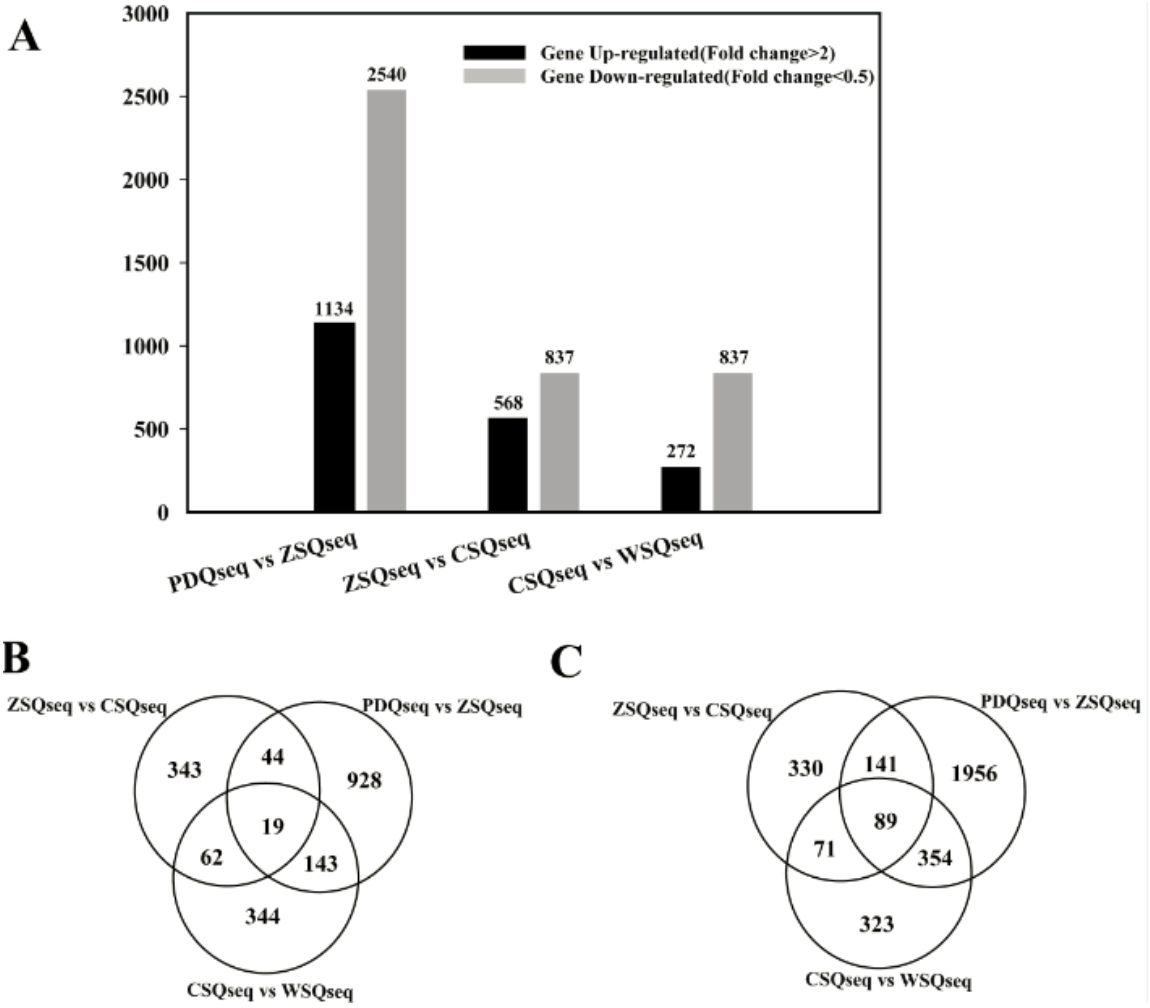


Figure 2

The sum the of genes with differentially expressed (DEGs) among PDQ, ZSQ, CSQ and WSQ of wampee fruit (A) and Venn diagram indicating the overlap of ascertained up-regulated (B) and down-regulated (C) DEGs among PDQ vs. ZSQ, ZSQ vs. CSQ and CSQ vs. WSQ.

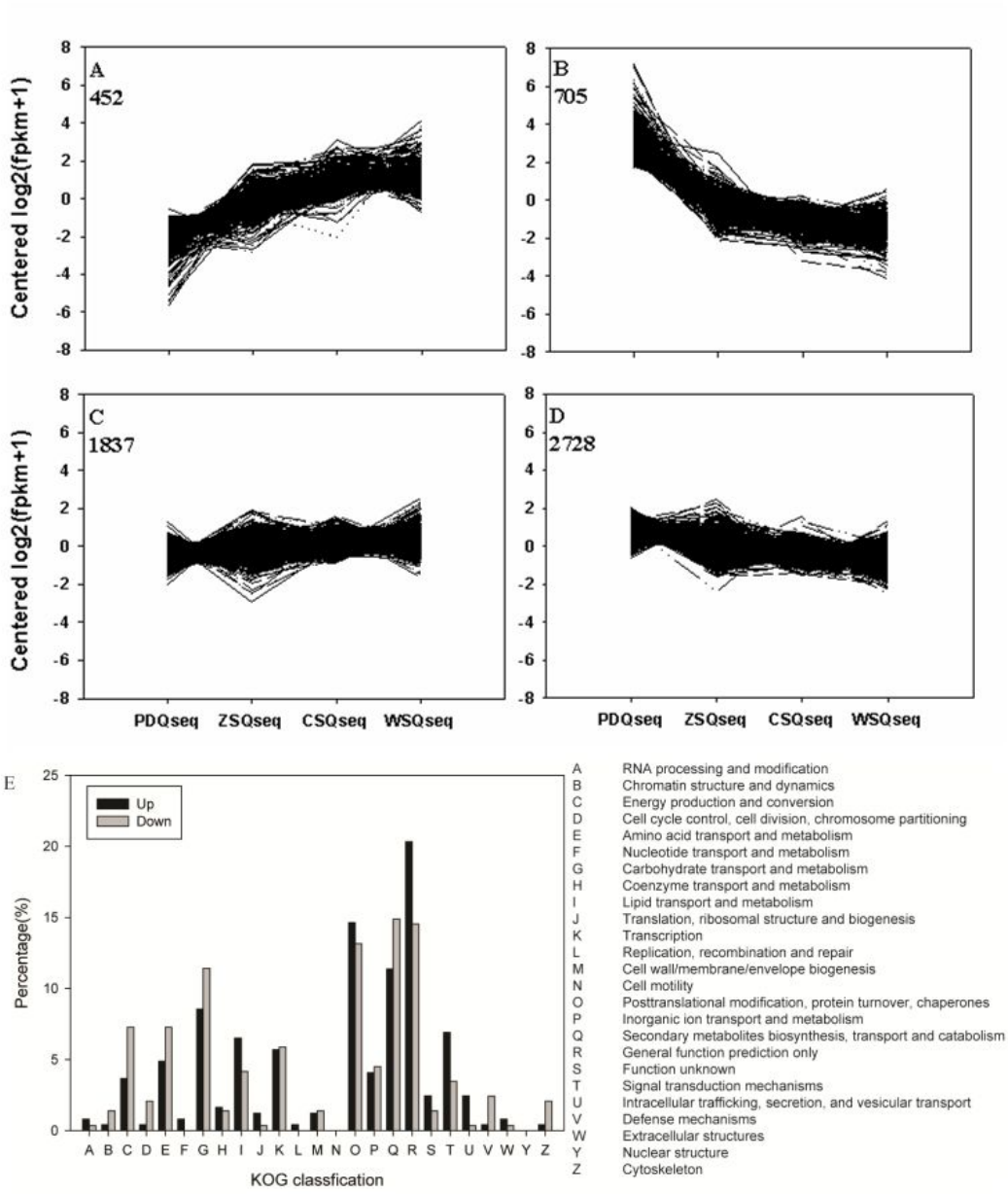


Figure 3

Expression profiles of the differentially expressed genes (DEGs) in steps of wampee fruit advancement and ripening. Four expression profiles are exhiited, with A and B showing genes with up-regulated and down-regulated expression, respectively, and C and D showing the irregular expression ones. KOG categorization was indicated for up and down regulated genes (E).

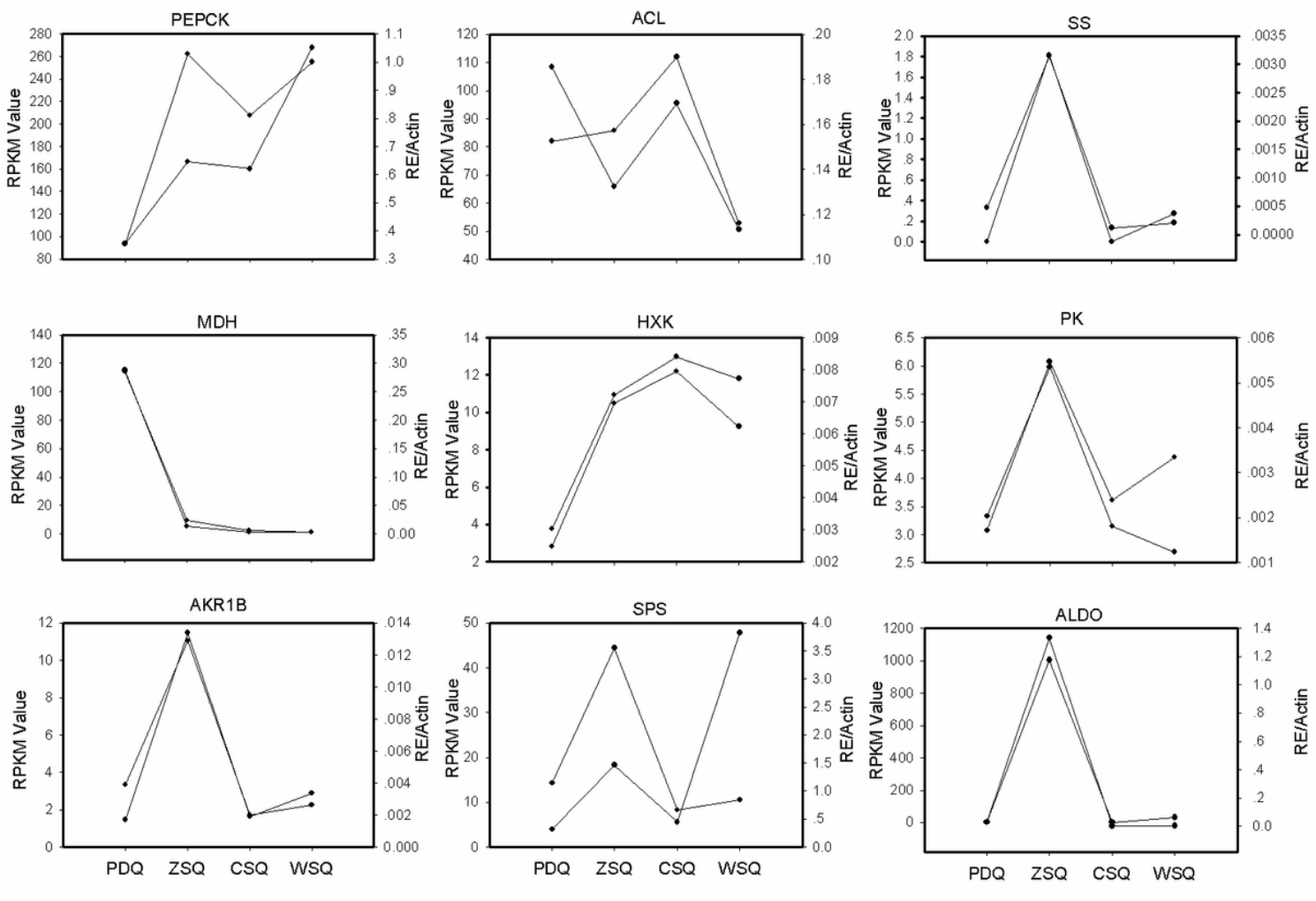


Figure 4

Transcript expressions of 9 selected genes attributed to citrate and sucrose metabolism evaluated via qRT-PCR.

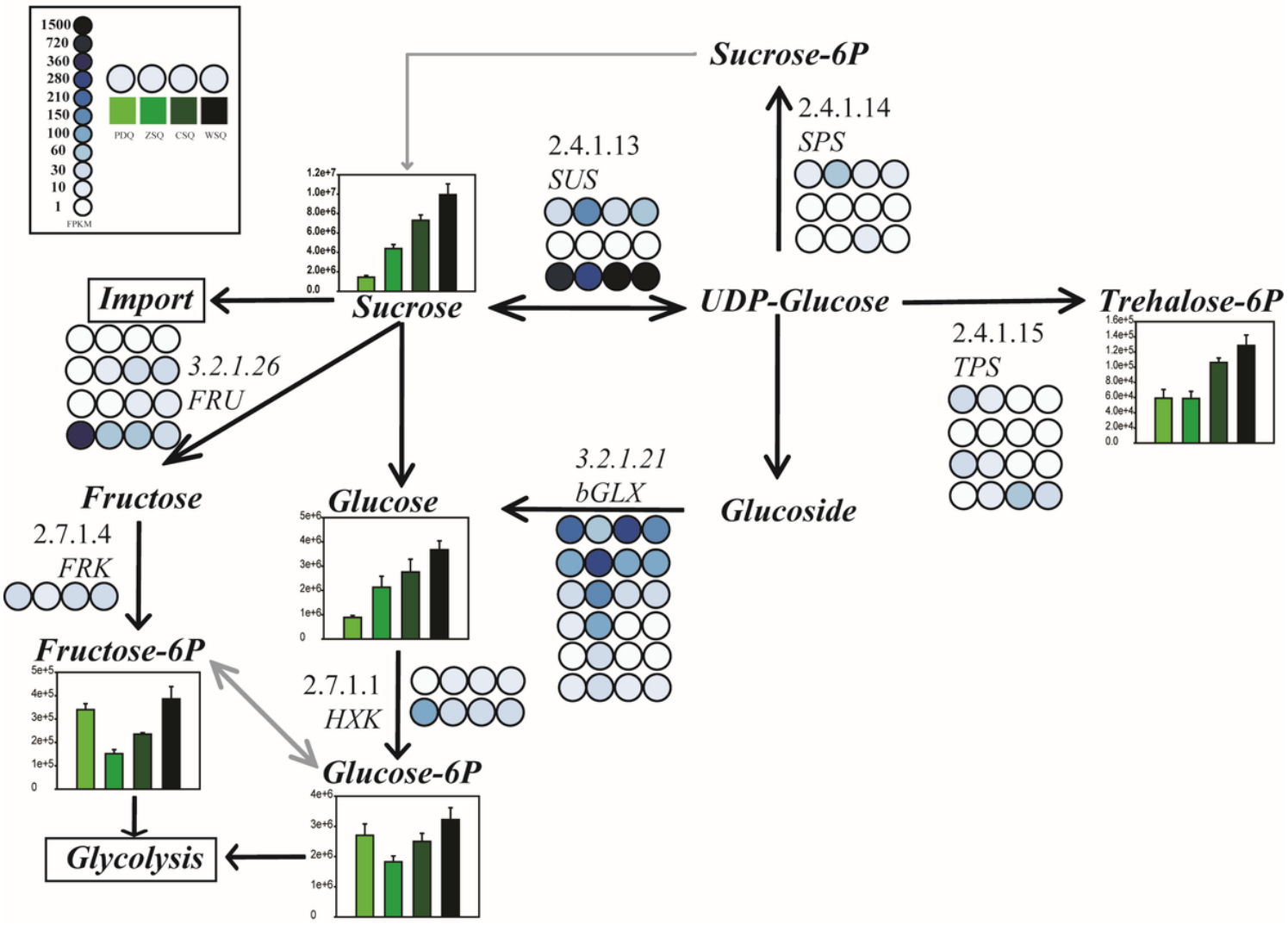


Figure 5

Regulation of sucrose metabolism trajectories during wampee fruit development and ripening. The contents of metabolites are exhibited in columns, whilst the expression values of genes are presented circles. The color from white to black displays the expression value from low to high. The expression trends were shown as RPKM.

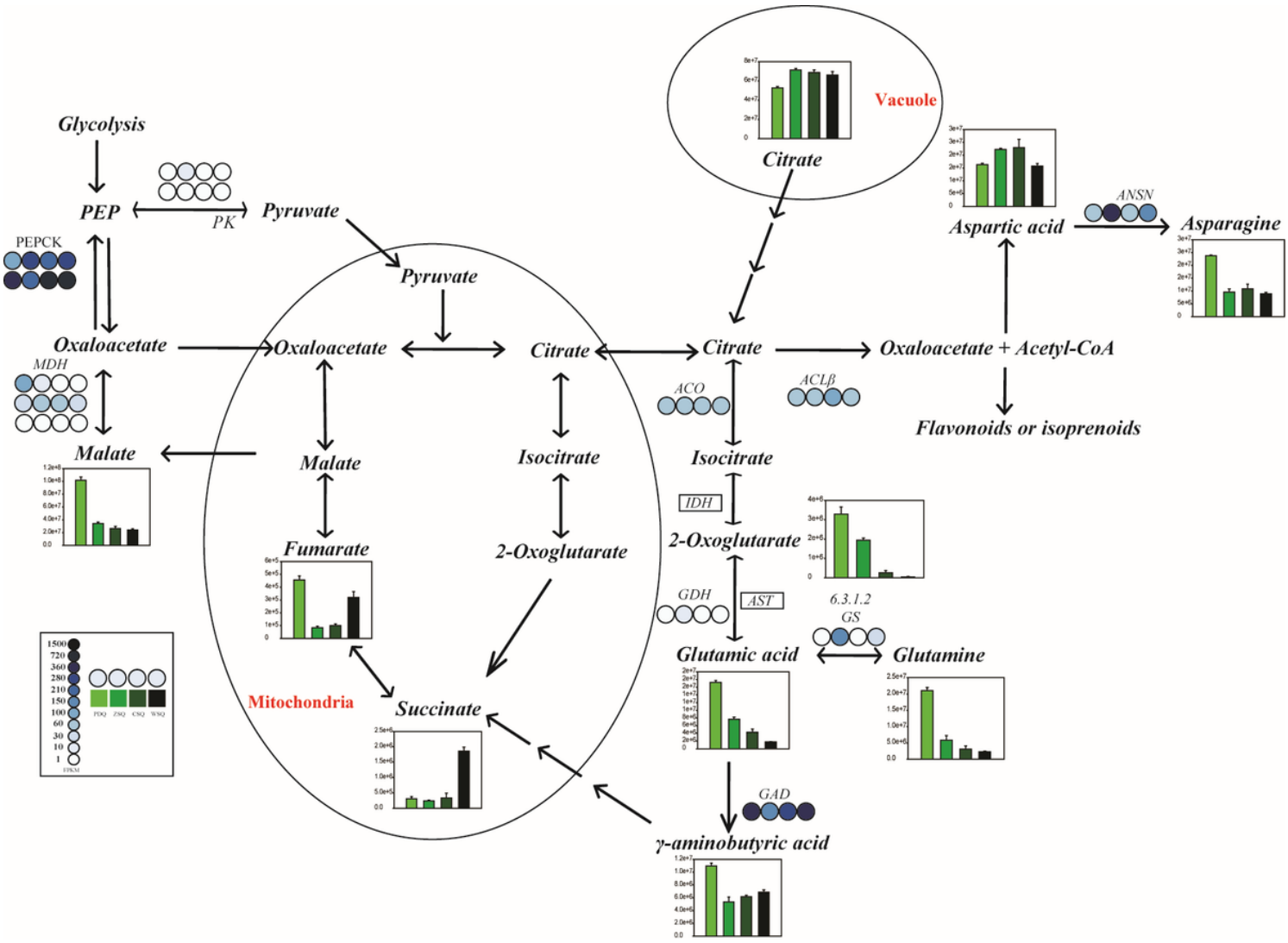


Figure 6

Regulation of citrate metabolism trajectories during wampee fruits advancement and ripening. The contents of metabolites are exhibited in columns, whilst the expression values of genes are presented in circles. The color from white to black displays the expression value from low to high. The expression trends were shown as RPKM.

Supplementary Files

This is a list of supplementary files associated with this preprint. Click to download.

- Supplement3PrimersofqPCR.xls
- Supplement2RPKMvaluesofallunigene.xls
- Supplement1Listof623metabolites.xlsx